

MECHANICAL PROPERTIES OF ALKALI-HALIDE CRYSTALS  
(NaCl, KBr, KCl)

J. K. GALT

TECHNICAL REPORT NO. 45

September 17, 1947

RESEARCH LABORATORY OF ELECTRONICS  
MASSACHUSETTS INSTITUTE OF TECHNOLOGY

The research reported in this document was made possible through support extended the Massachusetts Institute of Technology, Research Laboratory of Electronics, jointly by the Army Signal Corps, the Navy Department (Office of Naval Research), and the Army Air Forces (Air Materiel Command), under the Signal Corps Contract No. W-36-039 sc-32037.

MASSACHUSETTS INSTITUTE OF TECHNOLOGY

Research Laboratory of Electronics

Technical Report No. 45

September 17, 1947

MECHANICAL PROPERTIES OF ALKALI-HALIDE CRYSTALS

(NaCl, KBr, KCl)

by

J. K. Galt

Abstract

The pulse method has been applied to measure mechanical properties of NaCl, KBr and KCl at 10 and 30 Mc/sec. The elastic constants of KBr have been measured in the low-temperature region. An upper limit for the attenuation of shear waves in the 110 and 100 directions has been obtained. The strain-optical constants have been measured by a traveling-wave method suggested by Mueller.



# Mechanical Properties of Alkali-Halide Crystals

(NaCl, KBr, KCl)

## 1. Introduction

The availability of electrical circuits for pulsing has made possible the use of pulsed ultrasonic measurements for the determination of the mechanical properties of a medium. The present research is a survey of the usefulness of this technique for studying the properties of crystals of the alkali halides. Measurements have been made on NaCl, KBr, and KCl.

The first of the properties which we measure with this technique is the set of adiabatic elastic constants,  $c_{1k}$ . These are the proportionality constants between stress and strain in the material. They determine the velocity with which ultrasonic waves are propagated in the material, and it is from measurements of these velocities that we calculate the constants. The general expressions for the velocity of an ultrasonic wave in a crystalline material have been discussed by Shaefer and Bergmann<sup>1</sup>; the particular case of a cubic crystal has been developed by Mueller<sup>2</sup>.

The constants  $c_{11}$ ,  $c_{12}$ ,  $c_{44}$  of a cubic crystal are determined here from the velocity of three waves. The first is a compressional wave propagated along a cubic axis. Its velocity is  $\sqrt{c_{11}/\rho}$ , so it determines  $c_{11}$ . The second is a shear wave propagated along a cubic axis. Its velocity is  $\sqrt{c_{44}/\rho}$ ; it thus determines  $c_{44}$ . The third is a shear wave propagated in the 110 direction. Its velocity is  $\sqrt{(c_{11} - c_{12})/2\rho}$ , and together with a knowledge of  $c_{11}$  it determines  $c_{12}$ .

Some previous measurements of these constants have been made by Huntington<sup>3</sup> using this technique. Most of such measurements, however, have been made by means of the composite oscillator technique<sup>4</sup>.

The ratios of strain-optical constants  $p_{1k}$  may also be measured conveniently with the pulse technique. These constants determine the changes in the optical properties of a crystal when it is strained.

To define the strain-optical constants of a material we first define an index surface<sup>5</sup>. In general, this surface will be an ellipsoid whose equation we may write as:

$$a_{11}x^2 + a_{22}y^2 + a_{33}z^2 + 2a_{12}xy + 2a_{23}yz + 2a_{31}zx = 1. \quad (1)$$

The  $a_{1k}$  are constants which determine the direction and magnitude of the principal axes of the ellipsoid. Now in the case of an unstrained cubic crystal, the ellipsoid is a sphere, but when the crystal is strained, the surface is distorted. If we use superscript zeros for the  $a_{1k}$  in the unstrained case, we may write for cubic crystals:

$$a_{11}^0 = a_{22}^0 = a_{33}^0 = \frac{1}{n^2}; \quad a_{12}^0 = a_{23}^0 = a_{31}^0 = 0 \quad (2)$$

$$\dots \quad \frac{1}{n^2} (x^2 + y^2 + z^2) = 1.$$

Now for the  $a_{ik}$  in the crystal under strain we have in general:

$$\begin{aligned}
 a_{11} &= a_{11}^0 + p_{11}^x x + p_{12}^y y + p_{13}^z z + p_{14}^y z + p_{15}^z x + p_{16}^x y \\
 a_{22} &= a_{22}^0 + p_{21}^x x + p_{22}^y y + p_{23}^z z + p_{24}^y z + p_{25}^z x + p_{26}^x y \\
 a_{33} &= a_{33}^0 + p_{31}^x x + p_{32}^y y + p_{33}^z z + p_{34}^y z + p_{35}^z x + p_{36}^x y \\
 a_{23} &= a_{23}^0 + p_{41}^x x + p_{42}^y y + p_{43}^z z + p_{44}^y z + p_{45}^z x + p_{46}^x y \\
 a_{31} &= a_{31}^0 + p_{51}^x x + p_{52}^y y + p_{53}^z z + p_{54}^y z + p_{55}^z x + p_{56}^x y \\
 a_{12} &= a_{12}^0 + p_{61}^x x + p_{62}^y y + p_{63}^z z + p_{64}^y z + p_{65}^z x + p_{66}^x y
 \end{aligned}
 \tag{3}$$

In the cubic case, the symmetry is such that the matrix of the  $p_{ik}$ 's<sup>6</sup> is:

$$\parallel p_{ik} \parallel = \begin{vmatrix} p_{11} & p_{12} & p_{12} & 0 & 0 & 0 \\ p_{12} & p_{11} & p_{12} & 0 & 0 & 0 \\ p_{12} & p_{12} & p_{11} & 0 & 0 & 0 \\ 0 & 0 & 0 & p_{44} & 0 & 0 \\ 0 & 0 & 0 & 0 & p_{44} & 0 \\ 0 & 0 & 0 & 0 & 0 & p_{44} \end{vmatrix}
 \tag{4}$$

The ratio of  $p_{ik}$ 's determine the polarization of light diffracted by ultrasonics in a crystal. This fact permits us to measure  $p_{12}/p_{11}$  and  $p_{44}/(p_{11} + p_{12})$  by observing the polarization of light diffracted in this way. The method used here is that suggested by Mueller<sup>2</sup> (his method B).

The third mechanical property which is of interest is internal friction. Any mechanism for dissipating the energy in mechanical vibrations will produce an attenuation in the traveling ultrasonic wave. We may define such an attenuation by the relation

$$X = X_0 e^{-\alpha x}
 \tag{5}$$

where  $X$  is the stress amplitude of the wave,  
 $x$  is the distance traveled by the wave,  
 $\alpha$  is the attenuation constant.

We may measure  $\alpha$  here by measuring the variation in X with distance. Measurements have been made of the attenuations of each of the waves mentioned in connection with the elastic constants in NaCl, KBr and KCl. The values are so low, and vary among themselves so little, that it is felt that they represent merely an upper limit rather than an actual measurement. Beam spreading and other propagation factors probably cause most of their observed attenuations.

Lastly we are interested in the yield stress of these materials. This is the smallest stress which causes a permanent strain in the material. In particular, a shear in the  $1\bar{1}0$  direction in the  $110$  planes in these materials causes what is known as slip. Presumably such a yield stress would set an upper limit to the amplitude of a sound wave producing a similar stress which could propagate in the medium. It has been found that in the NaCl crystals used here, no such effect occurs when the stresses in the sound wave reach the static yield stress. The "dynamic" yield stress seems to be higher than the static value. This may have been caused by a hardening due to the presence of strains in the samples. We will discuss it again later.

## 2. Equipment

The experimental technique involved in making the measurements on sound propagation in these crystals is built around the use of pulses of sound. A quartz crystal is affixed to the surface of the alkali-halide crystal. Electronic circuits similar to those used for radar purposes during the war are designed to apply an r-f electrical pulse to the quartz, which, by virtue of its piezoelectric property, then radiates a pulse of mechanical vibrations into the alkali-halide crystal. This pulse travels back and forth through the sample, producing an echo in the form of an electrical signal each time it strikes the quartz. The echoes are presented on an oscilloscope, and the velocity and attenuation of the mechanical vibrations are determined from measurements made on these echoes. A block diagram of the equipment is shown in Fig. 1.

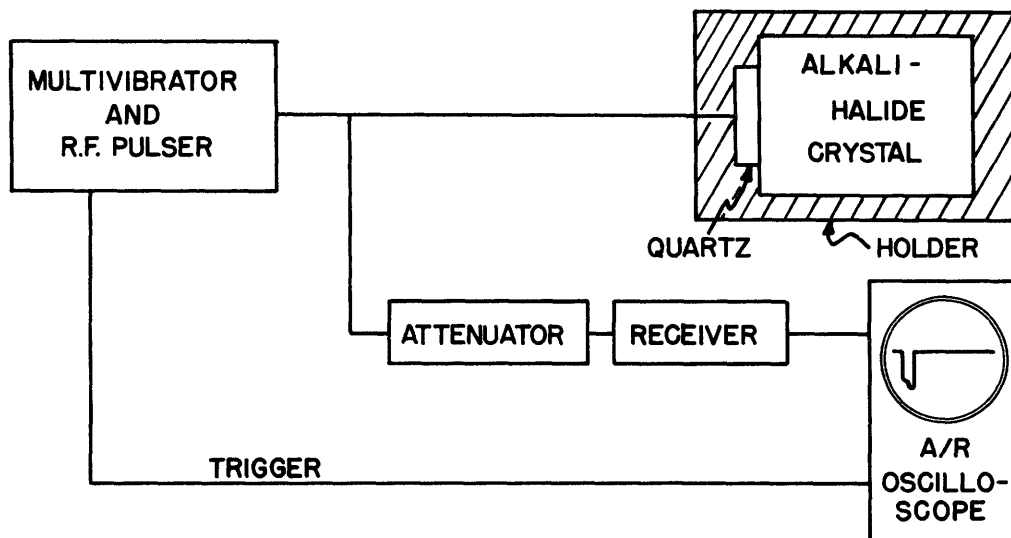


Figure 1. Block diagram of equipment.

A Dumont Type 256-B A/R Range Oscilloscope sends out d-c pulses, 1  $\mu$ sec long and of rectangular shape, which trigger the multivibrator and through it the r-f pulser. This circuit develops an r-f electrical pulse which is transmitted to the quartz. Some of this signal goes to the receiver too, of course. We will discuss this in more detail later (Sec. 3.) The quartz produces mechanical vibrations as mentioned above and these cause a series of echoes which are transmitted from the quartz to a receiver, through an attenuator, in the form of electrical signals. The output of the receiver is fed to an oscilloscope, and the echoes appear as deflections on the screen. A typical set of these echoes is shown in Fig. 2. We measure the ultrasonic path length in the sample, and the times at which these

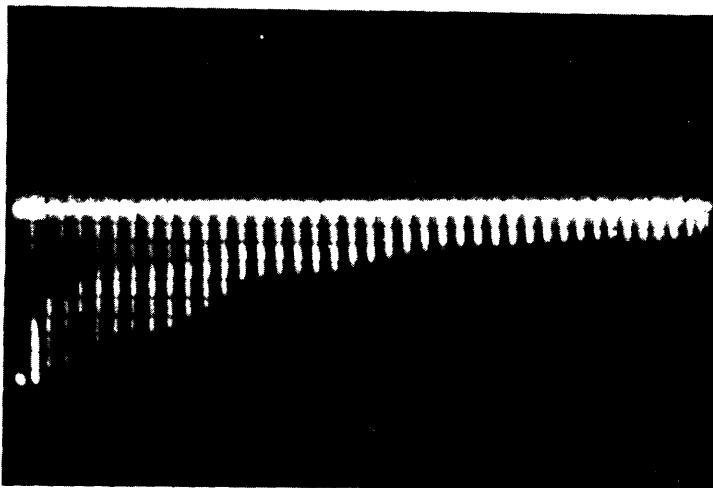


Figure 2. Successive echoes in NaCl block. Oscilloscope deflection is downward.

echoes occur so that we can plot distance traveled vs. time. The slope of this plot is the group velocity of the wave.\* The times at which the echoes occur are measured on the calibrated sweep of the A/R scope in exactly the same way as a radar measures the range of a target. The trigger which fires the transmitter and thus starts the whole sequence of events is synchronized with accurately spaced marker pips and with the oscilloscope sweep. The result is that the marker pips appear on the sweep and calibrate it so that time intervals may be measured quite accurately, (1/30  $\mu$ sec on one sweep, 1/3  $\mu$ sec on the other). The amplitudes of successive echoes are measured by reading on the attenuator the attenuation required to bring them to a constant level. From the amplitudes of the echoes and the distances traveled, we determine attenuation. These data must be interpreted rather carefully and we will discuss the procedure in more detail in Sec. 4.

Circuit diagrams of the multivibrator and r-f pulser and of the receiver are shown in Figs. 3 and 4. The Dumont Type 256-B A/R Range Oscilloscope used as a presentation unit is described in detail in the instruction book which accompanies it. No repetition of the material in that book will be attempted here since the circuit is rather involved and a complete discussion would take too much space. The instrument is especially useful for velocity measurements since the timing of the marker pips which calibrate the sweep is

---

\* No dispersion has been detected in these materials so that to the accuracy of the measurements at least, the group velocity is equal to the phase velocity.



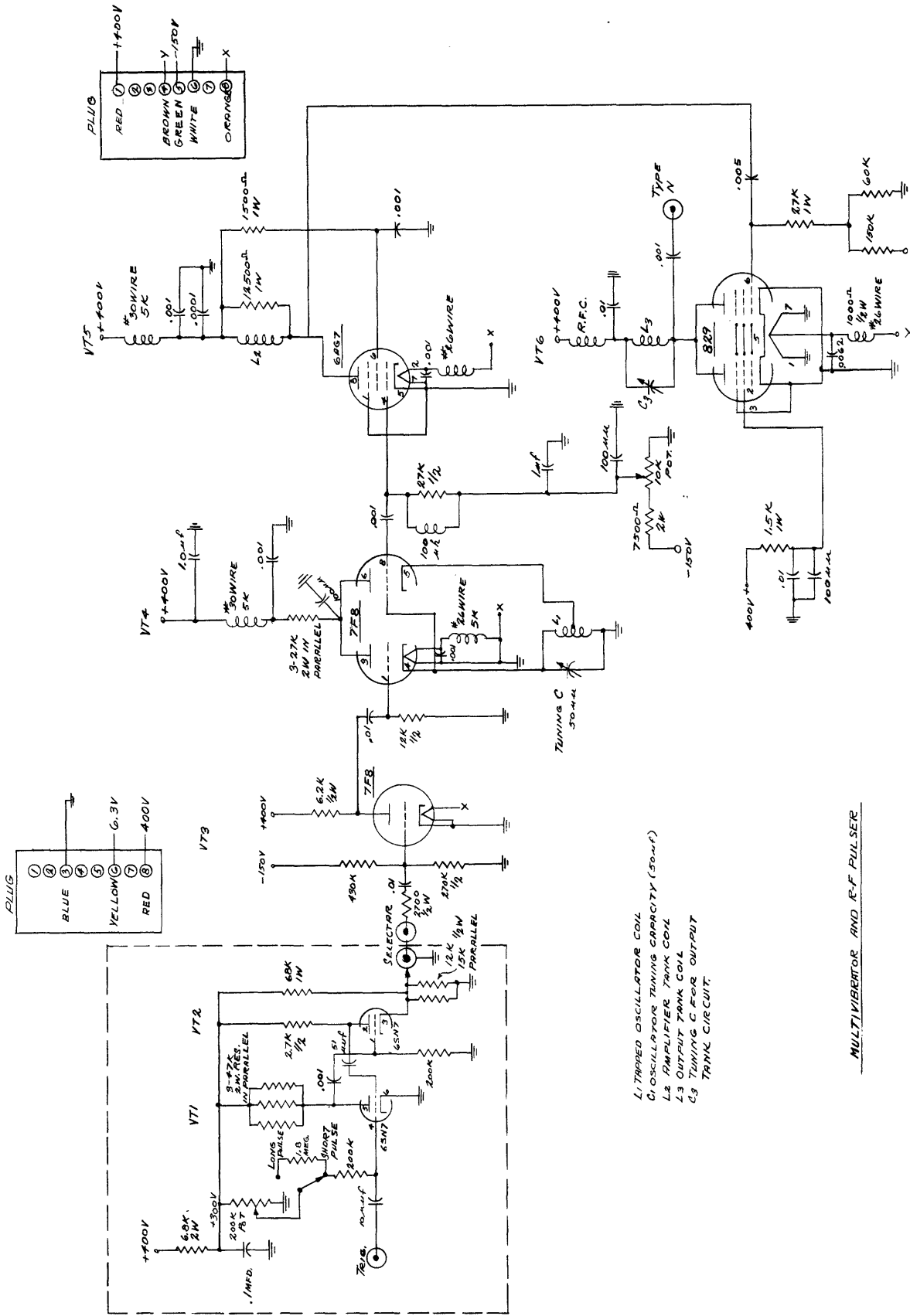


Figure 3. Multivibrator and r-f pulser circuit.

MULTIVIBRATOR AND R-F PULSER



synchronized with the frequency of a crystal. This means that the spacing between the markers is as accurate as the frequency of the crystal so that errors from this source are no larger than a few parts in  $10^5$ . Readings are taken from a helipot which can be calibrated by means of the markers to within one part in  $10^3$  or  $10^4$ , if sufficient care is taken. Two sweeps are used, one 122  $\mu$ sec long (20,000 radar range yards) and the other 1220  $\mu$ sec long (200,000 radar range yards). Small sections of these sweeps may be viewed in making an actual reading so that the accuracy to which the helipot may be read on the short sweep is about  $1/30$   $\mu$ sec, while on the long sweep, it is about  $1/3$   $\mu$ sec.

Some measurements were made at 30 Mc/sec also. The equipment used for this work was essentially identical with that used at 10 Mc/sec. Consequently, it will not be discussed in detail here except to say that the change in frequency is accomplished by merely changing the coils in the resonant circuits.

The three holders used in this work are shown in Fig. 5. The simplest, designated A in the figure, was designed for use at room temperature. The stem is a coax whose outer

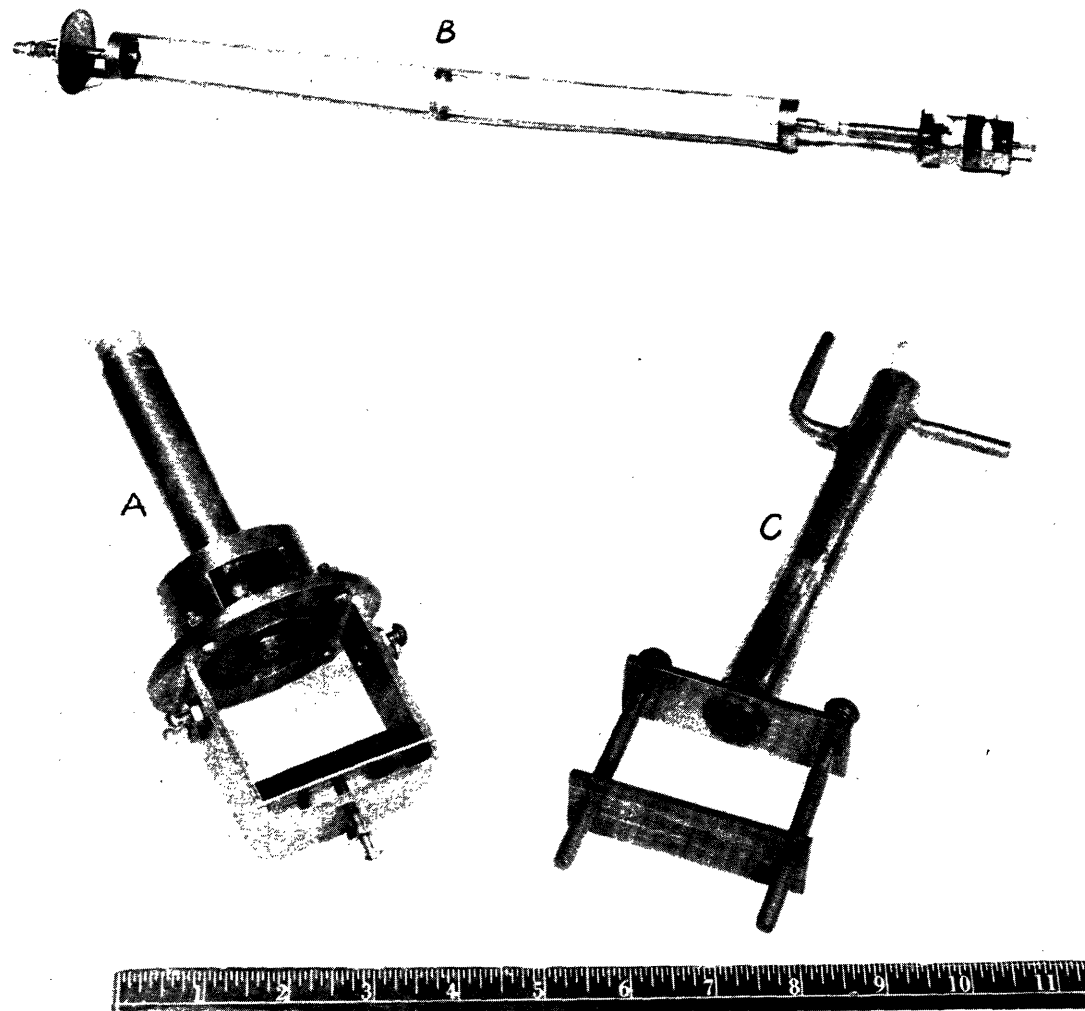


Figure 5. Holders (for samples).

conductor ends in a sylphon bellows and whose inner conductor is broad and flat at the end. Attached to this is a frame to support a machine screw which clamps the quartz against the end of the coax until contact is made with the inner conductor. At this point the sylphon is under compression. Some flexibility is given to the clamp by using a layer of sponge rubber in addition to a metal plate between the machine screw and the sample. A hole was cut in the sponge rubber so that only air was in contact with the alkali halide directly opposite the quartz, but in the author's opinion this was not necessary.

The other two holders are designed for different temperature ranges. The one marked B in Fig. 5 is used for measurements at temperatures as low as that of liquid helium. The coax has a springy center conductor as well as outer conductor in order that contact to the electrodes will be maintained at low temperatures even though the alkali halide contracts more than the brass of the holder. The long frame suspension is used to suspend the holder in the cold space of a Collins Helium Cryostat<sup>7</sup> for the measurements. The sample is packed in cotton and clamped in place on the sides in order to prevent the vibration in the cryostat from displacing it and thus breaking contact with the electrodes. A thermocouple is attached for measuring the temperature. The holder marked C in Fig. 5 is used for high-temperature work. All joints are welded and the coax center conductor is supported on glass beads. The center conductor is springy, but the spring is at the end away from the alkali halide in order to prevent excessive heating of it. No sylphon bellows may be used in this holder, of course, but the outer conductor is effectively sprung by means of springs on the two clamping screws. This holder is placed in an oven so that the end of the stem comes out to be connected to the electrical equipment. It has been used up to 400°C. Tubular connections are provided so that air cooling may be used to prevent the temperature at the r-f connector from becoming excessive.

A perspective drawing of the optical setup for measuring strain optical constant ratios is shown in Fig. 6. All equipment is mounted on a fairly heavy optical bench. The light source used is a Western Electric point-arc. It is small enough in dimensions so that no slit system is necessary. A condenser lens focuses the light from this source at infinity so that it forms essentially a parallel beam. This beam is polarized by a Glan-Thomson prism and then passes through the alkali-halide crystal. In the method used the plane of polarization makes an angle  $+45^\circ$  with the horizontal as determined by the optical bench. A film of a liquid whose index of refraction is exactly equal to that of the alkali halide is pressed against the sides of the sample with microscopic slides to minimize the scattering of light from the ground surfaces. The end of the sample is pressed up against a brass plate. In this way, the sample is held horizontal with respect to the optical bench so that the crystallographic directions are definitely determined with respect to the polarizer. The quartz is on the bottom side and the coax which connects to it also presses the sample against the top plate. The ultrasonic wave thus travels vertically up and down through the sample. The analyzer is mounted some distance (about 7 feet) further along the beam so that the diffracted images will be separated from the undiffracted image of the source. The images are observed with an eyepiece and the analyser is adjusted from these observations. Occasionally, the undiffracted image is blocked out by a fitting placed over

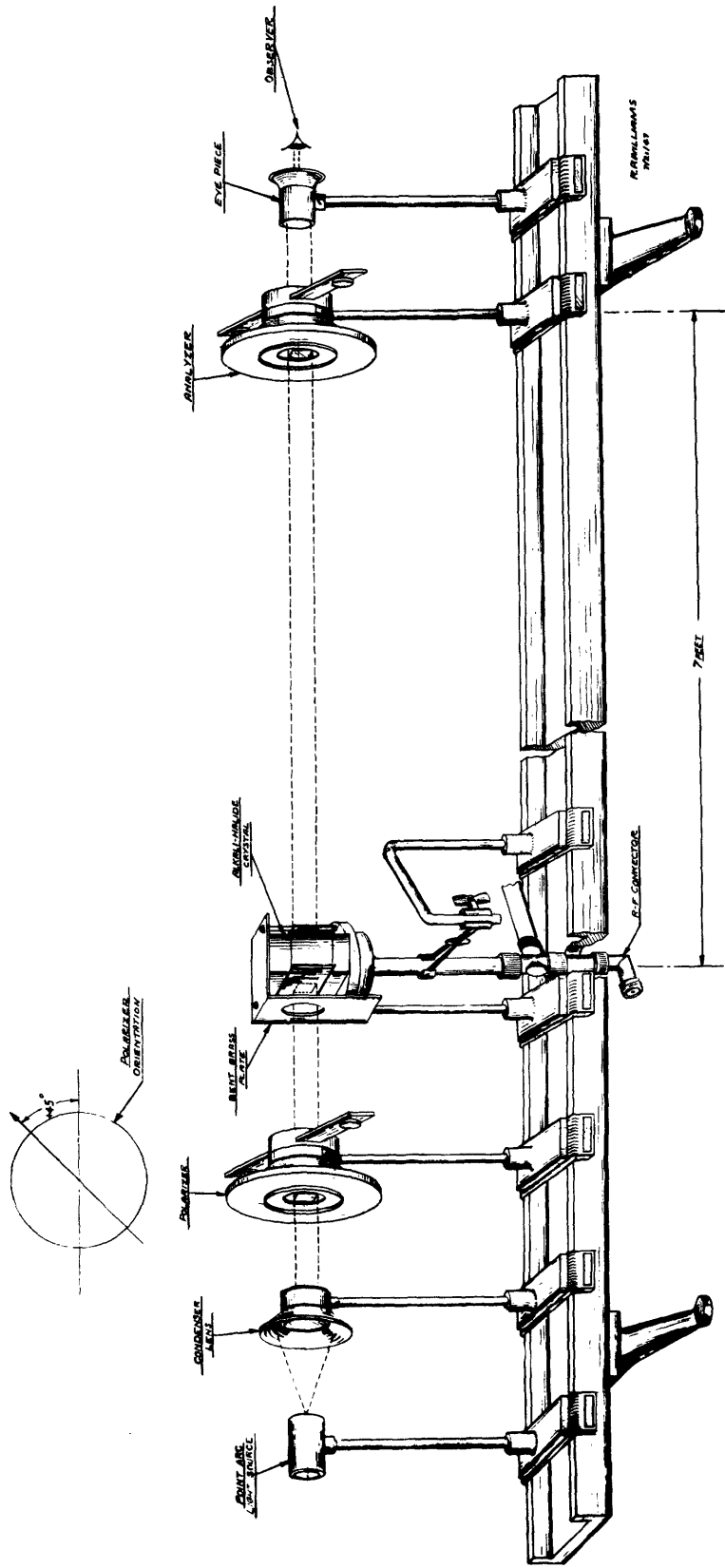


Figure 6. Equipment for measuring strain-optical constants.

the eyepiece. The main difficulty in making the readings, however, is scattered light which produces a background. The optical surfaces must be kept as clean as possible to minimize this.

### 3. Measurement Technique

Since the pulse techniques only recently became available, it seems desirable to give some discussion of the experimental methods used for this sort of work. A considerable part of this technique especially that used at room temperature, was developed by Dr. H. B. Huntington.

3.1. Quartz Orientation. In order to obtain waves which will be propagated in the desired direction, we must orient the crystal sample so that two faces are perpendicular to the desired direction of propagation. The desired wave in this direction may then be selected by affixing a quartz crystal to one of these faces with proper crystallographic orientation. When a compressional wave is desired, the face of an X-cut<sup>8</sup> quartz is simply affixed to that of the solid sample. For shear waves in the 110 direction, however, there are two possibilities. A Y-cut quartz is used, and the position of the x-axis of the quartz must be so oriented as to cause the desired wave. If the x-axis of the quartz is along the  $\bar{1}\bar{1}0$  direction in the sample, a wave of velocity  $\sqrt{(c_{11} - c_{12})/2\rho}$  is propagated. If it is along the 100 direction, a wave of velocity  $c_{44}/\rho$  is propagated. If it is between these two directions, both waves are propagated. The velocity of a shear wave along the 100 direction is independent of the direction of shear.

It should be noted that purely transverse and purely longitudinal plane waves are only propagated in the 100, 110, and 111 directions in a cubic crystal. The general problem of determining the character of the waves in a crystal has been solved by Shaefer and Bergmann<sup>1</sup>, and the special case of cubic crystals is discussed by Mueller<sup>2</sup>. They find that three waves may be propagated in any direction and that the displacement vectors of these three waves are mutually perpendicular. However, in cubic crystals, except for waves in the 100, 110 and 111 directions, one wave, which is called quasi-longitudinal, makes a small angle with the direction of propagation; at least one of the other two is quasi-transverse. The third may be transverse, but is usually quasi-transverse. Obviously, we cannot in general excite one of these waves alone with a quartz, no matter how it is oriented. We will get echo multiplication at all times and more pulse distortion.

3.2. Electrodes. The quartz crystals at the frequencies used here in general take the form of discs. Electrodes are plated on these discs in such a way that a coax pressed against one side may be used to excite them. This is done by bringing the coating on one side around the edge to the other side as described by Huntington<sup>3</sup>. An uncoated ring insulates the electrodes from each other. A coated crystal is shown in Fig. 7.

3.3. Films. In order to transmit vibrations from the quartz to the crystal sample, a film must be used to connect the two mechanically.

This problem has been quite satisfactorily solved at room temperature by using salol (phenyl ester of salicylic acid) as the cement. This was originally suggested by Mr. C. S. Pearsall of this Laboratory. It melts at 42°C, and crystallizes below that temperature.

The quartz and alkali halide are attached by warming them and the salol to about 45°C, placing a drop or two of the then liquid salol on the alkali halide, where the quartz is to be placed, lowering the quartz into place and letting the system cool while a small pressure (from a brass weight) is applied to the back of the quartz. The crystallized salol is quite rigid at room temperature even though this is not far below its melting point. This rigidity, of course, is extremely desirable if the film is to transmit shear waves.

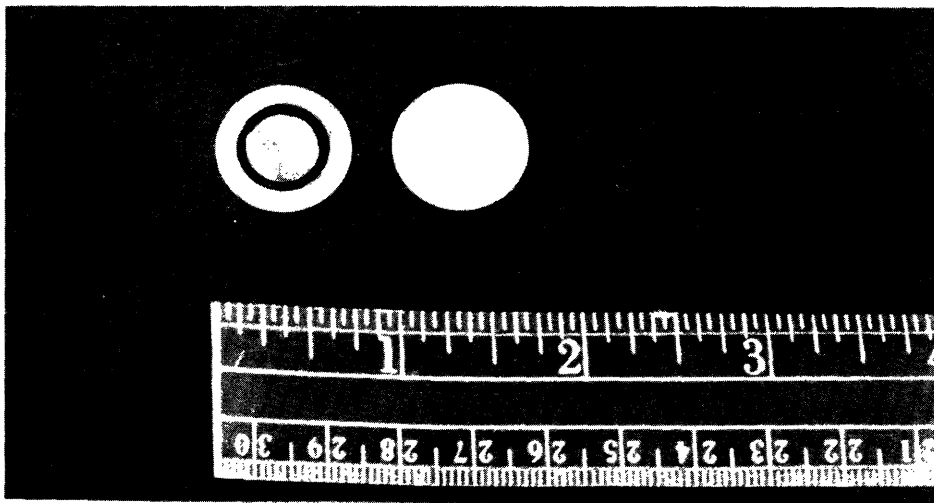


Figure 7. Electrodes on quartz crystals.

The problem of providing a film which will hold over a range of temperatures is considerably more complicated. The quartz and usually the film material itself has a smaller thermal expansion coefficient than that of the alkali halide. Consequently, as the temperature is lowered, the alkali halide contracts more than the quartz until the quartz, acting through the cement film, produces a tension on it. Since its breaking stress in tension is rather low, this often causes the alkali halide to crack. On the other hand, if the temperature is raised, the alkali halide is compressed by the quartz in the same way. It can stand much higher stresses in compression, and what usually happens as the temperature rises is that the film cracks off.

No one film is available which will solve this problem over the whole range of temperature. The best film for the low-temperature region found so far is essentially a stop-cock grease. It is a solution of natural (crepe or para) rubber(6 parts) in vaseline (60 parts). Such a mixture was suggested by Balamuth<sup>4</sup>. The optimum rubber concentration has not yet been found, but it is no larger than this and the author feels it may be lower. This film is rigid enough below 0°C to transmit shear waves. It is applied by putting a few spots of the grease on the alkali halide, putting the quartz on top, and then warming while a slight pressure is applied to the back of the quartz. The grease melts at 40 - 45°C sufficiently to distribute itself uniformly in a film between the quartz and the alkali halide. This grease freezes quite solid in the region

between 100°K and 200°K. In order to reduce the difference in the distances contracted by the two substances, the quartz is broken up into a mosaic of five or six pieces before it is cemented on. This makes it possible for motion of the pieces of the crystal to reduce the shearing action on the film to some extent. A picture of such a crystal cemented in place is shown in Fig. 8. Even with this arrangement, cracking occurs at

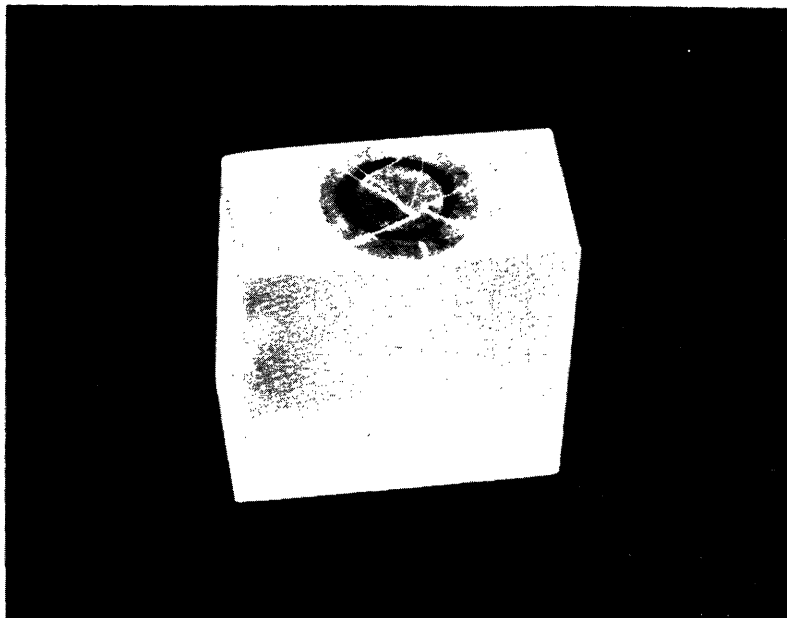


Figure 8. Broken quartz crystal in place on alkali-halide sample.

90°K or above. Measurements have been extended below this point for the waves propagated along the 100 direction. The cracks do not destroy echoes completely here. For waves propagated along 110, however, the cracks occur at 45° to the direction of propagation, and once they have occurred, the echoes pattern is destroyed completely. In passing, it may be mentioned that Rose's<sup>4</sup> technique of introducing a relatively strong metal whose expansion coefficient is near that of the alkali halide has disadvantages here because of the difference in the technique of measurement. The present technique requires a set of echoes due to successive trips of the sound pulse back and forth in the alkali halide. If we introduce another material between the quartz and the alkali halide, we also introduce another set of echoes. In order to distinguish the two sets, it is desirable to have the path in the metal long compared to the path in the alkali halide. If we wish to keep the total assembly size reasonable, this requires reducing the path length in the alkali halide and hence the accuracy of the method. It is possible, however, that this method could be used, after some experimentation, to avoid the cracking problem.

When the temperature is raised, the first difficulty to appear is the deterioration of the chemically deposited silver electrode coating. This makes it impossible to use for our purpose the water glass plus talcum powder cement which is often recommended in this temperature range since, when this cement is baked on as it must be, the electrode



on the quartz is destroyed. Obviously, it is desirable for the cement to conduct electrically so that it can form an electrode as well as bind the quartz to the alkali-halide crystal. All these requirements seem best met by the Hanovia Flexible Silver Coating No. 2. This is a suspension of silver-carrying material in an organic liquid. It is applied to the alkali halide, the quartz is broken into a mosaic and put down on top under mild pressure as before, and the system is baked at 150-160°C for three hours to remove the organic liquid and leave the silver material. The coat is brought around to the back side to act as a contact to the coax just as the chemically deposited coating does. This type of film has been used successfully up to 400°C. In the neighborhood of that point, the shearing action due to the differential contraction seems to break the bond with the alkali halide. The weakness of this bond in this case may quite possibly be due to the fact that the recommended bake-out temperature for this cement is 200°C and the temperature used was 150-160°C. The lower temperature was used to reduce the possibility that the sample would crack in tension on being cooled to room temperature after the baking process was over and before the measurement run could be made.

It should also be pointed out that this film problem can be solved over a large temperature range for compressional waves by using liquids. This procedure is quite satisfactory if the system does not have to be placed in a vacuum as it does in a helium cryostat of the Collins type<sup>7</sup>. Such a reduction in pressure will tend to cause liquids to boil away although one may pick liquids non-volatile enough so that this will not be disastrous.

3.4. Impedance Matching. In measuring attenuations, no appreciable amount of the energy should be allowed to drain off when the ultrasonic wave in the medium is reflected from the quartz. This means that the mechanical impedance presented by the quartz to the wave each time it returns must be very different from the characteristic impedance ( $\rho v$ )<sup>\*</sup> of the sample material. The wave must see a large mismatch every time it strikes the quartz. On the other hand, we also wish to introduce large signals into the sample to see if we can produce stresses with the ultrasonic signal as large as the yield stress or at least large enough to produce a change in the strain-optical pattern. This can only be done if the same two impedances, that of the quartz and that of the sample, are matched at least when the signal from the transmitter comes through. We are therefore faced with the problem of the transmit-receive (TR) box in radar work. The problem of adjusting these impedances has not been solved in a completely satisfactory way, but some progress has been made and this work will be described here.

This problem is easily solved for the low-level measurements by making the impedance of the electrical circuits placed across the quartz very low. The value used here is 75 ohms since that is the characteristic impedance of the attenuator. This is much lower than the impedance of the quartz loaded on one side with an alkali halide as the ones used here are. Consequently, while the r-f electrical pulse does not cause a very large sound pulse, once the sound pulse has been generated in the alkali halide, no appreciable amount of the signal is drained off when it strikes the quartz after reflection from the other end of the sample. A smaller impedance than 75 ohms seems to be desirable.

---

\* where v is the velocity of the wave involved.

30 Mc/sec, but in any case, the sensitivity of the receiver is such that the echoes can easily be picked up under these conditions. Receiver sensitivity is of the order of  $10^{-14}$  watts. We may diagram the circuit connections here as in Fig. 9.

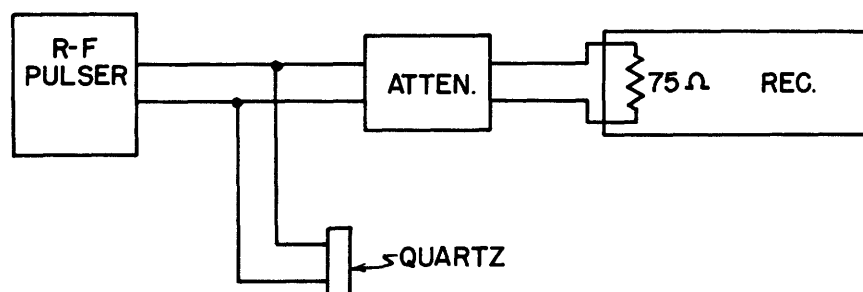


Figure 9. Block diagram of connections used for low-level measurements.

This solution does not work satisfactorily if it is necessary to raise the signal level. In order to do this with a pulser of reasonable size and without elaborate insulation arrangements at the quartz, the internal impedance of the pulser must be matched to that of the quartz. When this is done, a large fraction of the energy in the mechanical vibrations is drained off on each reflection. This makes it impossible to observe attenuations directly, but changes in attenuation with signal level or temperature may be observed from changes in the ratios of the echo amplitudes to the signal developed by the r-f pulser. These can be observed by connecting the plates of a synchroscope across the electrodes on the quartz. The receiver input impedance must also be made large enough so that the pulser output is not dissipated in it. This problem can theoretically also be solved by the use of a suitable T-R arrangement, as in a radar set, but no such arrangement suitable for this purpose is known to the author.

**3.5. Impedance Measurement.** In order to determine the acoustic signal power from the r-f voltage, we must know the impedance of the quartz crystal. A simple measurement with a Q-meter while the quartz is affixed to the alkali halide is not satisfactory because it is a c-w measurement and the absorption of sound in the alkali halide is so small that the sample acts as an acoustic resonator. The readings then do not reflect the impedance which

determines the behavior of the quartz in pulsed operation where these resonant effects do not enter. Upon searching the tabulated values in the literature, it appeared that Pb, which has such a large attenuation that it cannot act as a resonator, has a  $\rho v$  for shear waves approximately equal to that for NaCl. Since we are interested primarily in shear waves for attenuation measurements, the Pb was substituted for the NaCl in making the impedance measurements, and the curve of Fig. 10 was obtained in the neighborhood of 10 Mc/sec.

Some further comments on the impedance of quartz may be made. The data in Fig. 10 indicate a minimum shunt impedance of approximately 10,000 ohms in the neighborhood of 10 Mc/sec. These data could be checked by placing resistances in parallel with the quartz and noting the effect on pulse amplitude. This was done and the values obtained substantially check those given in Fig. 10. Measurements on the Q-meter were not so reliable at 30 Mc/sec, but the value obtained was in the neighborhood of 1000 ohms there. It is felt that this explains a slightly faster decline in echoes obtained at that frequency.

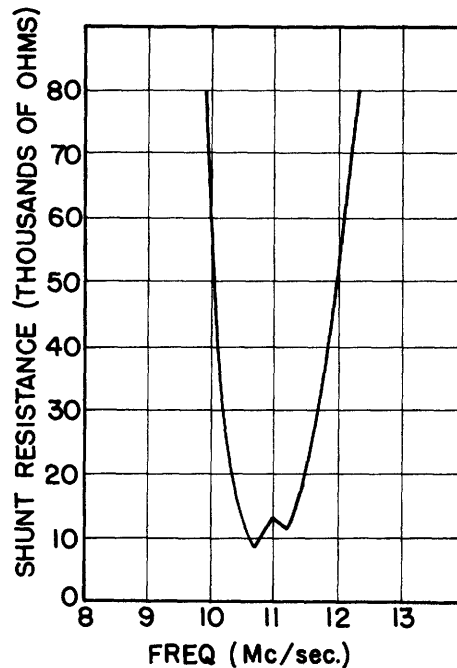


Figure 10. Plot of shunt resistance vs. frequency for quartz crystal affixed to Pb.

3.6. Strain-optical Constant Measurements. The technique of measuring the strain-optical constant ratios involves first reading the angle at which the polarizer crosses out the first-order diffraction image of a slit. The equipment has been described in Sec. 2. For most of the readings, the image to be crossed out was invisible for an appreciable interval (up to 2 or 3 degrees). Consequently, the position of crossing was measured by measuring the angles at which the image disappeared on each side and using a value half way between these two. Extreme care is necessary on the part of the observer to find these two points. It is sometimes necessary to disregard readings which deviate a great deal

from the average, as sometimes the eye tires enough to fail to detect a faint image. Even though liquids whose index is matched to that of the alkali halide were used to prevent light scattering by the walls of the sample, the light scattering in the system produced a background which increased the difficulty of making the readings.

One further point may be mentioned with respect to the strain-optical constant measurements. The diffraction of an appreciable amount of the incident light requires a sound wave of large amplitude traveling back and forth in the alkali halide a large part of the time. This was accomplished by triggering the r-f pulser at a high rate (4000 times a second) and increasing pulse length until the pulses almost overlapped. Under these conditions, the diffracted light was quite adequate for the measurements. Under favorable conditions, second and third diffraction orders appeared.

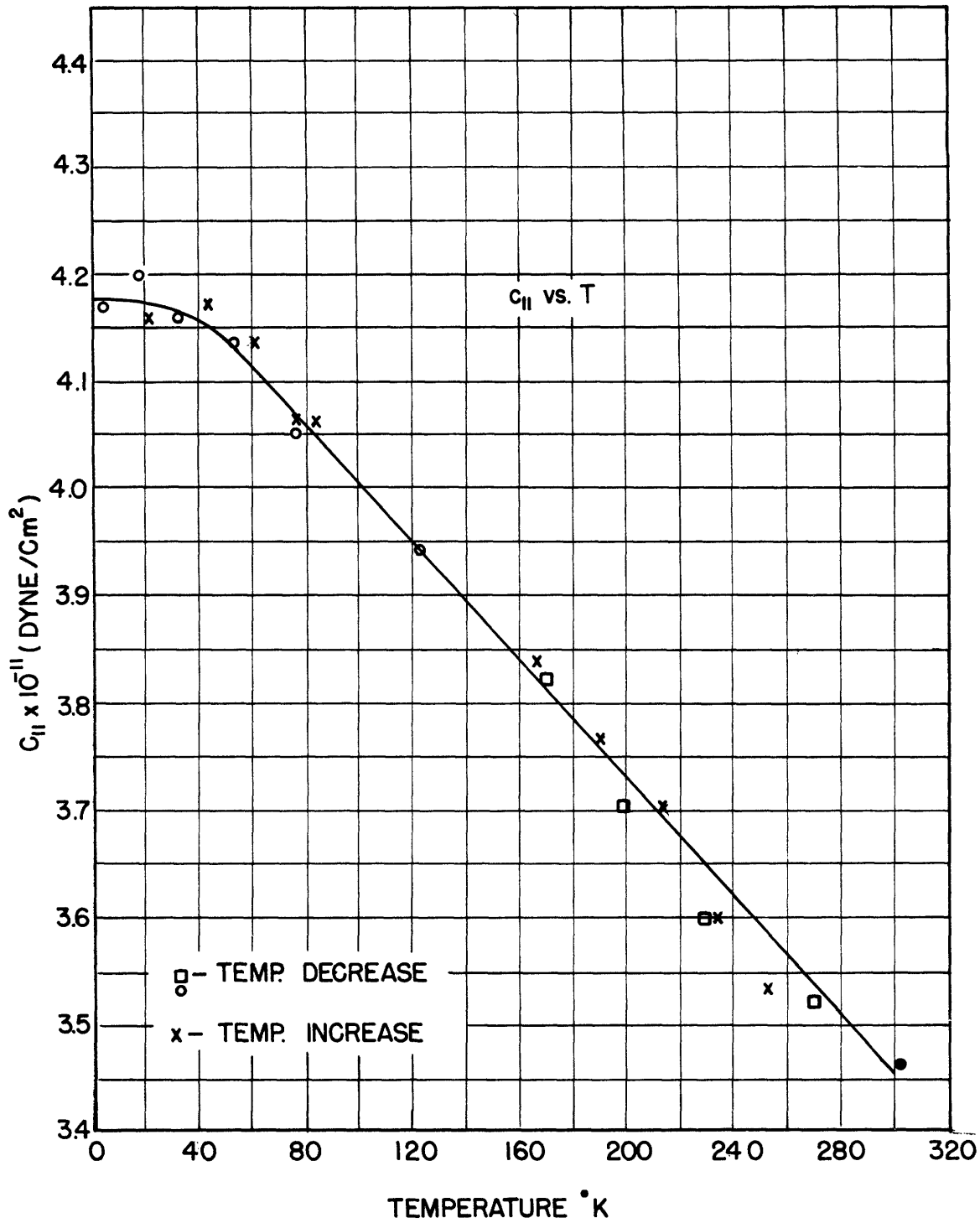
#### 4. Results

4.1. Elastic Constants. Table I gives the adiabatic elastic constants measured at room temperature. The measurements of Huntington<sup>3</sup> and Durand<sup>4</sup> are presented for comparison.

Table I. Elastic Constants Measured at Room Temperature (Units are dynes/cm<sup>2</sup>).

		NaCl	KBr	KCl
$c_{11} \times 10^{-11}$	Galt	4.87	3.46	3.98
	Huntington	4.85	3.45	
	Durand	4.99		4.08(280°K) 4.00(300°K est)
$c_{12} \times 10^{-11}$	Galt	1.24	0.58	0.62
	Huntington	1.23	0.54 ± 0.03	
	Durand	1.31		0.6
$c_{44} \times 10^{-11}$	Galt	1.26	0.505	0.625
	Huntington	1.26	0.508	
	Durand	1.27		0.634(280°K) 0.63(300°K est)

Some of the factors which may introduce errors have been mentioned earlier. The path over which the measurement is made may be measured as accurately as desired by means of micrometers. These are easily checked by means of size blocks. The error from this source is no larger than one part in  $10^4$ . Similarly, the marker spacing is accurate to a few parts in  $10^5$ . The sweep must be calibrated in terms of these markers with some care, however, and this calibration must be checked from time to time as it tends to drift slightly with time. It is difficult to reduce errors from this source below 1 part in  $10^3$ , although it can be done if the calibration is made frequently enough and with sufficient care. The most important difficulty, however, arises from the pulse distortion. Only data on the earlier echoes are used, but in spite of this precaution errors of 3 to 5 parts in  $10^3$  are quite apt to arise from this source. It is felt that errors in the tab-



ulated values of  $c_{11}$  and  $c_{44}$  are no more than 1 per cent and are usually less than this. Errors in  $c_{12}$  thus may be larger, since it is derived by subtracting two measurements.

The elastic constants of KBr have also been measured over the range of low temperatures. The constants  $c_{11}$  and  $c_{44}$  have been measured down to 4.5°K;  $c_{12}$  has been measured down to only 138°K for reasons which will be discussed below. A plot of  $c_{11}$  vs. T is shown in Fig. 11. The expanded scale was chosen in order to show clearly the flattening off at 0°K, although this scale rather over-emphasizes the scatter of the experimental points. Plots of  $c_{44}$  and  $c_{12}$  vs. T are shown in Fig. 12.

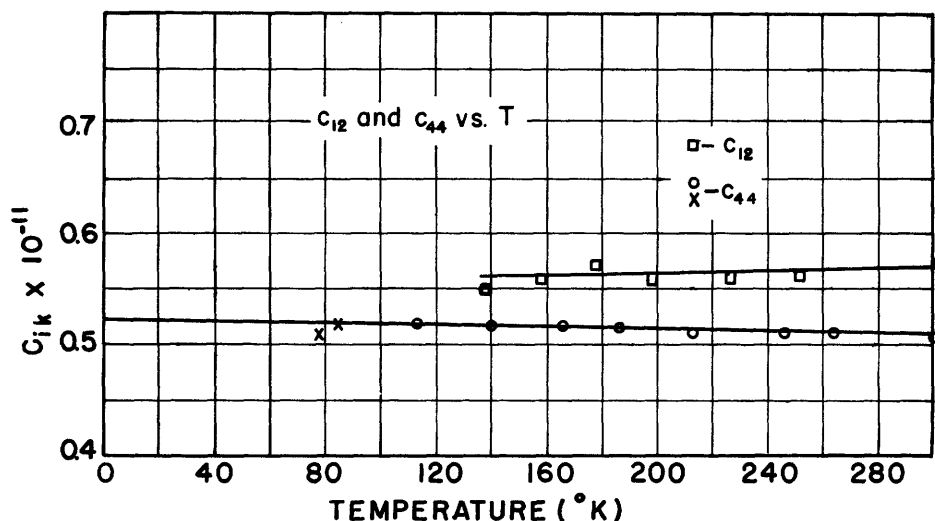


Figure 12.

The precision of the velocity measurements down to 100-120°K is essentially that of the room-temperature measurements. Some additional uncertainty in the points shown in Fig. 11 is introduced by the uncertainty in measuring temperature, however. Gradients several degrees in magnitude occur in the cryostat with the result that the thermocouple readings are not accurate measures of the average temperature over the volume of the sample. In addition, of course, there is some uncertainty in the calibration and reading of the thermocouple itself. The readings are checked with a helium gas thermometer in the cryostat for temperatures below 200°K. Above this, there is no check on the thermocouple. The thermocouple was calibrated at the temperature of dry ice (dry ice and acetone bath 195°K) and that of boiling nitrogen (77°K). A substantial part of the scatter of the points in Fig. 11 above 200°K is attributable to this difficulty. The stopcock-grease type of film used in these measurements (see Sec. 3) introduces some amplitude fluctuations in the pulses as the temperature changes because of the adjustments necessary when differential contraction between quartz and sample is taking place. These fluctuations do not alter the elastic constant measurements, however. Some additional pulse distortion may occur, especially at the higher temperatures with shear waves but it is not serious and it is not felt that the elastic constant measurements are in error by more than the 1 per cent estimated for the room-temperature measurements. Additional

errors are introduced into the plots of Figs. 11 and 12 by the uncertainty in the temperature measurement (approximately 5°K). It should also be mentioned that temperature readings on 4 points which are plotted as squares in Fig. 11 were taken on a thermocouple displaced from the sample, and the values plotted had to be reconstructed from the time-temperature curve of previous runs. Thus the points plotted as crosses are somewhat more reliable. It will be noted, however, that there is no systematic deviation between the sets of points.

In the 100-120°K neighborhood, the differential contraction always produces cracking in the KBr sample. When  $c_{11} - c_{12}$  was being measured, the wave travelled in the 110 direction while the cracks occurred along cleavage planes which were at 45° to the 110 direction. Such cracks completely eliminate echoes. The result is that measurements of  $c_{12}$  stopped when the sample cracked. When measurements on  $c_{11}$  and  $c_{44}$  were made, cracking also occurred, but the waves were travelling in the same direction as most of the cracks with the result that although some pulse distortion, and therefore some scattering in the data, occurred, echoes continued to come through and measurements could be made. Cracks sometimes occurred which were normal to the direction of propagation since this is also a cleavage direction but these merely introduce extra echoes. If they eliminate the echo from the end of the sample, these extra echoes themselves may be used for the actual measurement. A crack occurred during the  $c_{44}$  measurements which was used for this purpose. The crack was not along a perfect plane as might be expected so that some pulse distortion was produced and the path length was slightly uncertain so that the absolute value of the readings shows an error (as measured from the points plotted) of approximately 2 per cent. However, it was only necessary to use these measurements to determine the change in  $c_{44}$  below 110°K, and we are justified in extending the previous straight line on this basis although the curve must flatten out near 0°K. In this connection, it is important to note that while the estimated error in the absolute value of  $c_{44}$  in Fig. 12 is 1 per cent, changes smaller than this can be measured and the slope of the plot of  $c_{44}$  is fairly accurate, as the data plotted indicate.

As with the room-temperature measurements, the error in  $c_{12}$  may be larger than that in  $c_{11}$  and  $c_{44}$ . Deviations from a constant value for  $c_{12}$  in the data plotted cannot be considered as accurately established by these data. The plot indicates strongly that the Cauchy relation ( $c_{12} = c_{44}$ ) does not hold even at 0°K. This relation is derived on the basis of central forces in the crystal and the plot in Fig. 12 seems to mean that in KBr the forces are not central, but come closer to it as the heat vibrations die out.

It will be noted from Figs. 11 and 12 that the derivative of all the elastic constants of KBr with respect to temperature is zero at 0°K. This is especially noticeable in the plot of  $c_{11}$  vs. T. That this should always be so may be seen from the third law of thermodynamics. If we consider a plane compressional wave in the 001 direction, one of the Maxwell relations in thermodynamics gives us:

$$\left. \frac{\partial X}{\partial T} \right|_X = \left. \frac{\partial S}{\partial X} \right|_T \quad (6)$$

From the third law of thermodynamics we may write:

$$\left. \frac{\partial S}{\partial x_x} \right|_T = 0 \text{ at } 0^\circ\text{K} \quad (7)$$

so that

$$\left. \frac{\partial x_x}{\partial T} \right|_{x_x} = 0 \text{ at } 0^\circ\text{K}. \quad (8)$$

But since

$$\frac{\partial c_{11}}{\partial T} = \frac{\partial^2 x_x}{\partial T \partial x_x} = \frac{\partial}{\partial x_x} \left[ \left. \frac{\partial x_x}{\partial T} \right|_{x_x} \right], \quad (9)$$

we have

$$\frac{\partial c_{11}}{\partial T} = 0. \quad (10)$$

4.2. Strain-optical Constants. Table II gives strain-optical constant ratios and an estimate of the errors in the two ratios which were measured. The estimate cannot take into account inaccuracies caused by the permanent strains present in the alkali-halide crystals, of course, but it is felt that these are quite small. There were no very large strains present. Pockel's values for NaCl and KCl are presented for comparison.

Table II. Strain-optical Constant Ratios

Substance	$\frac{P_{12}}{P_{11}}$	$\frac{P_{44}}{P_{11} + P_{12}}$	$\frac{P_{44}}{P_{11}}$
<u>NaCl</u>			
Galt	$1.35 \pm 0.03$	$-0.042 \pm 0.004$	-0.099
Pockels	1.30	-0.0343	-0.079
<u>KCl</u>			
Galt	$0.76 \pm 0.01$	$-0.069 \pm 0.004$	-0.12
Pockels	0.74	-0.069	-0.12
<u>KBr</u>			
Galt	$0.77 \pm 0.01$	$-0.067 \pm 0.005$	-0.12



The principal source of error in determining  $\gamma_m$ , the difference in the angle of extinction between the diffracted and undiffracted light, is in reading the angular position of the analyzer at which the diffraction image disappears. In addition to this, uncertainty in the polarizer setting with respect to the crystallographic axes of the alkali-halide crystal may also cause an error. The crystal position is determined, as we mentioned above by the bent brass plate used as a holder. It is felt that errors in analyzer position from this source are 10 minutes or less since this uncertainty is only indirectly able to cause an error in  $\gamma_m$ . The uncertainty in the reading of the extinction angle can only be estimated on the basis of the spread in the data. Estimates have been made for each ratio on the basis of the data taken on it.

The light source used in taking the data on NaCl and KBr was a mercury arc. Since filtering to obtain a monochromatic source did not seem to affect the readings noticeably, an incandescent source, being more convenient, was used to take the KCl data. This is the arrangement shown in Fig. 6.

The values shown in Table II are quite consistent with the predictions of Mueller's theory.<sup>9</sup>

4.3. Attenuations. The method used here for making attenuation measurements is quite satisfactory if the attenuation is fairly large, as it is in liquids. If, however, the value of  $\alpha$  is smaller than about 0.01, it is apt to be obscured by the decrease in signal due to beam spreading and other propagation factors in a finite sample.

Measurements of attenuation of the same three waves used in measuring elastic constants have been made. The results are shown in Table III.

Table III. Attenuations Measured at Room Temperature.

Substance	Wave		Block Cross section cm	$\alpha(\text{cm}^{-1})$
	Prop. Dir.	Shear Dir.		
NaCl	110	110	4.06 x 2.31	0.0041
	100	010	4.05 x 2.2	0.0046
	100 (compressional)		4.03 x 2.2	0.0017
KBr	110	110	3.72 x 2.02	0.0043
	100	010	4.48 x 2.34	0.0048
	100 (compressional)		4.48 x 2.34	0.0011
KCl	110	110	4.12 x 1.87	0.0040
	100	010	4.19 x 2.10	0.0054*
	100 (compressional)		4.19 x 2.10	0.0034*

\* It is felt that these values are slightly high because the surfaces between which the waves travelled were not quite parallel.

The shear wave in the 110 direction was chosen because it causes a stress of the type required for static slip; it was thought that such a wave might show increased attenuation. This obviously does not occur.

It is clear that the attenuations obtained here are in the range where propagation factors are apt to obscure the attenuation. The data itself are so constant with respect to changes in crystallographic direction and material that it is felt that they can only be considered upper limits. The reduced values for the longitudinal waves suggest that scattering from permanent strain centers may be one cause for these values. The fact that essentially the same values were observed for 30-Mc/sec vibrations in NaCl, however, makes this hypothesis seem doubtful.

All values of  $\alpha$  in Table III are averages over at least 100 cms of travel of the wave, since detailed structure in the envelope of the echoes would introduce a large error if an appreciably smaller distance of travel were used.

Low-level attenuation of the shear wave propagated in the 110 direction in NaCl was also measured as a function of temperature up to 400°C. The silver coating and high-temperature holder mentioned in Sec. 3 were used. Small effects could not be observed because the envelope of the echoes was affected as the film adjusted itself to the differential expansion between the quartz and the NaCl, but no large attenuations were introduced at this temperature. It was thought that perhaps the yield stress would have decreased enough at this temperature so that even at these signal levels slip would be produced. This does not seem to occur.

The measurements made at high signal level are more crude than the low-level measurements, because no satisfactory T-R arrangement has been found. The ratios between the input pulse and the echoes, especially the first, were measured. A change in these ratios as the signal level is changed would presumably indicate a change in attenuation. A change of perhaps 2 db is caused by the changing impedance of the r-f pulser as signal level changes, so we can only observe fairly large effects this way. But if the large stresses in the wave produce slip, we should expect a large attenuation and therefore a large change in this ratio. Again, no effect was observed. Observations were made on NaCl and KBr. From the impedance and the r-f voltage, measured as described in Sec. 3, the acoustical signal power was determined. From this, and the radiating surface of the quartz, the stress produced in the sound beam could be obtained from the relation

$$\gamma = \frac{x^2}{2\rho v} \quad (11)$$

where

$\gamma$  is the sound intensity in watts/cm<sup>2</sup>

$x$  is the peak stress in the wave.

$\rho$  is the density of the material.

$v$  is the sound velocity.

The maximum stresses produced in these experiments were slightly larger than the static yield stress of NaCl (0.2 kg/mm<sup>2</sup>). The fact that no appreciable attenuation and therefore

presumably no slip occurred at these stresses has no obvious explanation except that the effective yield stress in these samples must be higher than the measured static value.

During these high signal level experiments, the alkali-halide crystals were observed through crossed polaroids. The strain-optical pattern observed in this way changed slightly in one case; a slight annealing action seemed to have been produced. This was not reproducible in other samples, however, and its relation to slip phenomena is not clear. Even after some annealing, there were permanent stresses in these samples. It is possible that these produced an increased yield stress in them.

The author wishes to express his gratitude to Professor H. Mueller for his help and advice in carrying out this research. He also wishes to thank Professor D. C. Stockbarger for providing the crystals on which this research was performed.

### References

1. C. Shaefer and L. Bergmann, Abh. Preuss, Akad. Wiss. phys.-math. Kl. 14, 222(1935).
2. H. Mueller, Zeitschrift für Kristallographie (A) 99, 122-41 (1938).
3. H. Huntington, "Ultrasonic Measurements on Single Crystals", M. I. T. RLE Technical Report No. 10, March 21, 1947; also Phys. Rev., 72, 321 (1947).
4. L. Balamuth, Phys. Rev. 45, 715 (1934); F. E. Rose, Phys. Rev. 49, 50 (1936); M. A. Durand, Phys. Rev. 50, 449 (1936); Hunter and Siegel, Phys. Rev. 61, 84 (1942).
5. M. Planck, "Introduction to Theoretical Physics", Vol. 4, Macmillan, New York, 1932, p.130.
6. F. Pockels, "Lehrbuch der Kristalloptik", Teubner, Leipzig, (1906) p. 480.
7. S. Collins, Rev. Sci. Inst. 18, 157 (1947).
8. W. G. Cady, "Piezoelectricity", McGraw-Hill, New York (1946).
9. H. Mueller, Phys. Rev. 47, 947 (1935).